

PROGRESS REPORT ON THE SLD ČERENKOV RING IMAGING DETECTOR*

V. ASHFORD,[†] T. BIENZ, F. BIRD, G. CRAWFORD,[†] M. GAILLARD, G. HALLEWELL, D. LEITH,
Y. KWON, D. MCSHURLEY, A. NUTTALL, G. OXOBY, B. RATCLIFF, R. REIF, D. SCHULTZ, H. SHAW,

S. SHAPIRO, E. SOLODOV,[§] N. TOGE, J. VA'VRA, S. WILLIAMS

Stanford Linear Accelerator Center, Stanford University, Stanford, CA 94305

D. BAUER, D. CALDWELL, A. LU, S. YELLIN
University of California, Department of Physics, Santa Barbara, CA 93106.

M. CAVALLI-SFORZA, P. COYLE, D. COYNE, E. SPENCER
Santa Cruz Institute for Particle Physics, University of California, Santa Cruz, CA 95064

R. JOHNSON, B. MEADOWS, M. NUSSBAUM

University of Cincinnati, Department of Physics, Cincinnati, OH 45221

1. ABSTRACT

We describe test beam results from a prototype Čerenkov Ring Imaging Detector (CRID) for the SLD experiment at the SLAC Linear Collider (SLC). The system includes both liquid and gas radiators, a long drift box containing gaseous TMAE and a proportional wire chamber with charge division readout. Measurements of the multiplicity and detection resolution of Čerenkov photons, from both radiators are presented. Various design aspects of a new engineering prototype, currently under construction, are discussed and recent R&D results relevant to this effort are reported.

2. INTRODUCTION

The SLD was designed to be a state-of-the-art detector to fully exploit the physics potential of the SLAC Linear Collider (SLC).¹ Particle identification is crucial to this objective. The Čerenkov Ring Imaging Detector (CRID) will provide almost complete particle identification over $> 90\%$ of the solid angle. In particular, $\pi/K/P$ separation will be possible up to about 30 GeV/c. Good e/π separation is also provided up to 5 GeV/c. Above this momentum the SLD calorimetry becomes effective at e/π separation.

Within the CRID (Fig. 1), UV Čerenkov photons, generated by the passage of charged tracks through both liquid and gaseous radiators, are directed onto the fused silica windows of the drift boxes. These photons produce electrons by ionization of a photo-sensitive vapor within the drift boxes. After drifting, the photo-electrons are detected by a proportional wire plane. Charge division along the sense wires

provides the conversion depth of the photon, while the drift time and wire number give its longitudinal and transverse position. This technique has been demonstrated by the CRID²⁻⁵ and DELPHI prototypes.⁶ Section 3 of this report summarizes recent results obtained with our physics prototype on the Čerenkov angle resolutions and the number of photoelectrons detected, for both the liquid and gas rings.

Tetrakis dimethylamino ethylene (TMAE) is the photosensitive vapor used within our drift boxes. Because of its very low ionization energy (5.36 eV), it has a good photoionization quantum efficiency in the 6 - 7 eV region. However, contamination in the TMAE, generated in the manufacturing process and from subsequent oxidation, impairs the CRID operation both by absorbing the UV photons and by capturing the drifting electrons. In Section 4 we describe our procedure for cleaning the TMAE and measuring its purity.

The current stage of our research and development program involves the construction of a barrel prototype whose design, materials and construction techniques will be as similar as possible to that proposed for the SLD CRID barrel. Successful construction and operation of this prototype pose a number of challenges in the areas of high voltage, materials, and monitoring. Section 5 of this report describes the recent technical progress in these issues.

3. THE PHYSICS PROTOTYPE

3.1 Construction

The "Physics Prototype" incorporates the essential features of the SLD design (described in more detail in Section 2)—liquid and gaseous radiators, spherical mirrors, a photosensitive drift box with its associated proportional wire chamber and operation above room temperature operation. Figure 2 is a schematic drawing of the device. Light from a 1.27 cm thick

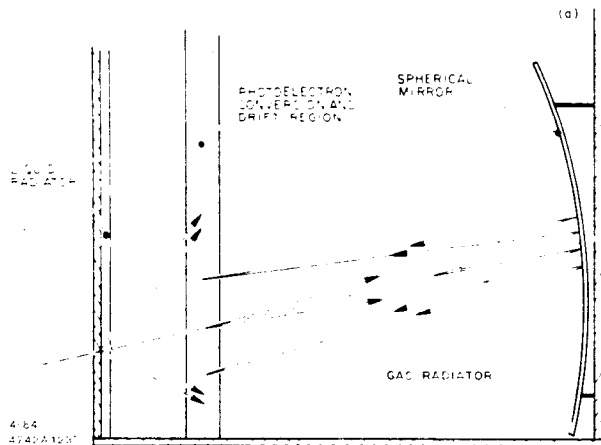


Fig. 1. The CRID principle for a two-radiator system.

* Work supported by the Department of Energy, contracts DE-AC03-76SF00515 and DE-AT03-79ER70023 and by the National Science Foundation under Grants PHY85-12145 and PHY85-13808

† Present Address: Biology Dept., University of California, San Diego, La Jolla, CA 92093

‡ Present Address: Dept. of Physics, Cornell Univ., Ithaca, NY 14853.

§ Permanent Address: Institute of Nuclear Physics, Novosibirsk 630090, USSR.

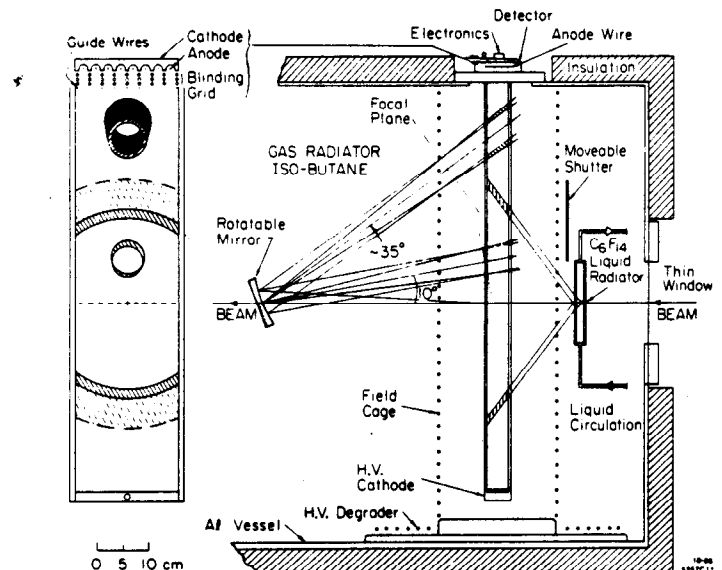


Fig. 2. Schematic of the Physics Prototype.

perfluoro-n-hexane¹³ (C_6F_{14}) liquid radiator ($n = 1.277$ at $\approx 2000\text{\AA}$) was "proximity focused" onto the upstream window of the drift box. A spherical mirror, tilted at 12.5° , focused the Čerenkov light developed within an atmospheric isobutane radiator ($n = 1.00157$ at $\approx 2000\text{\AA}$) onto the opposite window and away from the ionization deposited by the charged tracks. The drift box was 80 cm long, 20 cm wide and 4.5 cm thick. It was operated at a drift field of 400 V/cm. The drift gas was a mixture of 80% methane/20% ethane bubbled through TMAE at 28°C .

The detector design, shown in Fig. 3, was optimized to reduce the correlated backgrounds from the conversion of secondary U.V photons liberated in the avalanches at the sense wires. This was achieved by stringing the 64 sense wires within a "scalloped" cathode structure; this reduces the solid angle available for the "photon feedback" process. A further reduction was achieved by the introduction of blinding wires. With this design we observed less than 0.08 feedback photons per single electron avalanche.

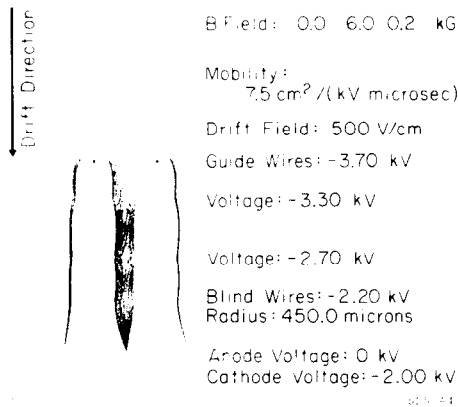


Fig. 3. Electrostatic simulation of the detector with a three layer blinding scheme.

To provide the position measurement in the depth coordinate, essential for the reduction of parallax broadening on the ring images, the sense wires were read out in a charge division mode. To reduce Johnson noise, high resistance carbon sense wires were used. The wires were $7\ \mu\text{m}$ in diameter, 6 cm long and had a resistance of about $25\ \text{k}\Omega$. Twenty of these wires, at $3.175\ \text{mm}$ pitch, were read out via LeCroy HQV810 based preamplifiers and shaping stages into LeCroy 2241 image chamber analysers. The estimated overall thermal noise with this system is ≈ 1500 electrons. This corresponds to charge division resolution of $\approx 2\%$ in position along the wire.⁷

3.2 Results

In February 1986, data were taken with a 11 GeV/c hadron beam mainly consisting of pions with a small kaon and proton component. Beamline Čerenkov counters were used to identify the beam particle.

Figure 4(a) shows an accumulation of 1500 pion gas radiator rings projected onto the mirror focal plane. Figure 4(b) shows the same plot using the depth information. The radial distributions of these electrons, shown in Figs. 5(a) and 5(b), clearly demonstrate the improvement in resolution obtained using the charge division technique. A similar improvement was also observed for the liquid ring. Table I summarizes the resolutions obtained for the liquid and gas rings and compares them with Monte Carlo calculations. Reasonable agreement is found.

The distribution of the number of photoelectrons contributing to each pion gas ring is shown in Fig. 6. It is well fit by a Poisson distribution with a mean of 8.6. Correcting for the incomplete coverage of the gas ring, the known losses due to the electron lifetime and the photoconversion depth gives

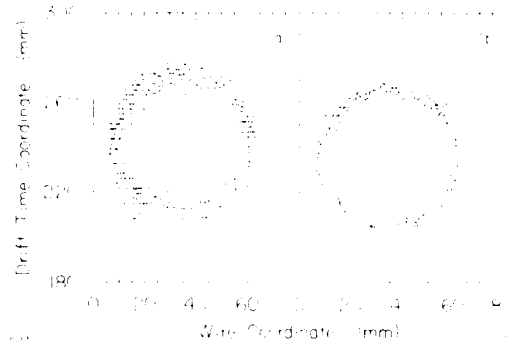


Fig. 4. (a) Gas radiator Čerenkov ring images for multiple events with parallax uncorrected, and (b) with parallax corrected using the depth coordinate obtained from charge division along the wire.

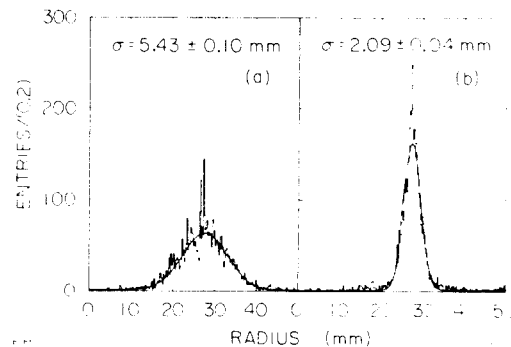


Fig. 5. Radial distributions for (a) the parallax uncorrected and (b) the parallax corrected pion gas rings.

Table I. Liquid and Gas Resolutions

	$\sigma_{p.e.}$		σ_{track}	
	Observed	Monte Carlo	Observed	Monte Carlo
Gas	4.3 mr	4.5 mr	1.4 mr	1.2 mr
Liquid	9.5 mr	8.0 mr	1.6 mr	1.6 mr

11.1 electrons on a ring, corresponding to an N_0 of $85\ \text{cm}^{-1}$. The corrected number for the kaons is 3.3 ± 0.3 . As the protons were below the gas threshold no electrons were expected and none were observed.

For the pion liquid ring, based on the number of electrons observed in the front arc we expect 34 ± 3 electrons in the full ring, corresponding to an N_0 of $86\ \text{cm}^{-1}$.

By fitting the pion and kaon gas rings to circles, we obtain the excellent π/K separation shown in Fig. 7.

4. TMAE STUDIES

To achieve satisfactory electron attenuation lifetimes, typically $50\ \mu\text{s}$, it was necessary to purify the TMAE and use only TMAE compatible construction materials within the drift box and the gas system.

Commercial TMAE⁹ contains about 3% impurities, 99% of which consists of the following components: Dimethylamine (DMA), Tetramethylhydrazine (TMH), Bis(dimethylamino)-methane (BMAM), Dimethylformamide (DMF), Tetramethylurea (TMU), and Tetramethyloxamide (TMO). Of these,

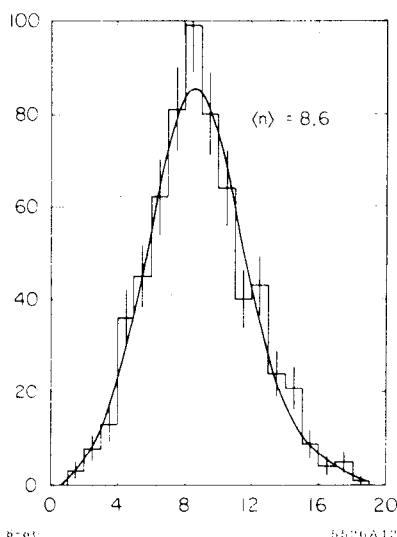


Fig. 6. The number of observed photoelectrons per pion gas ring fitted to a Poisson distribution of $\langle n \rangle = 8.6$.

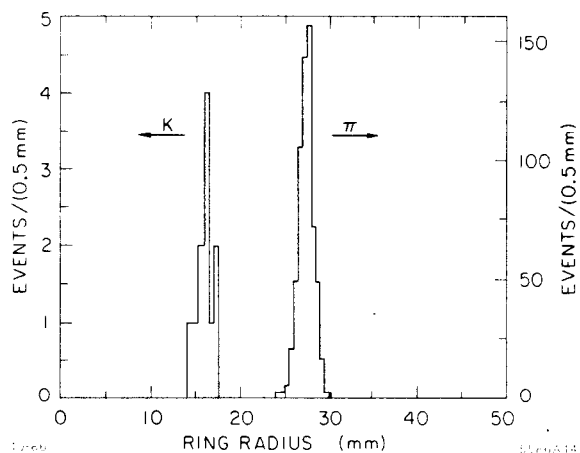


Fig. 7. Fitted ring radii for the kaon and pion events.

DMA is a strong absorber of UV photons, while TMO and TMU have high electron capture cross sections relative to oxygen. Removal of these impurities is essential for good UV photon detection. We have therefore adopted some of the techniques developed by Holroyd and collaborators:¹⁰ *i.e.*, TMAE is (1) washed in deionized water, then (2) dried on molecular sieves, (3) filtered through silica gel, and (4) vacuum distilled. We have analysed samples of TMAE after each successive step with Gas Chromatography/Mass Spectroscopy (GC/MS) techniques and measured the concentration of impurities.¹¹ We find that the first two steps reduce impurities to less than 0.4%, a level which appears adequate for CRID work.

In addition to the GC/MS measurements we have also used a monochromator to measure the UV absorption spectra of TMAE as a function of bubbler temperature. The measurements are shown in Fig. 8 and are in good agreement with measurements made by the OMEGA group.¹² The absorption lengths are expected to depend on temperature according to the Clausius-Clapeyron equation,

$$\mu(\lambda) = \mu_0(\lambda) \exp \left[-\frac{L_0}{R} \left(\frac{1}{300} - \frac{1}{T} \right) \right] \quad (1)$$

where μ is the inverse absorption length at temperature T , μ_0 its value at 300K, L_0 the latent heat of vaporization and R the gas constant. Figure 9 is a plot of the data at 1800Å

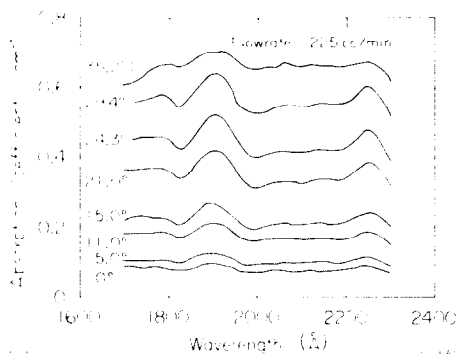


Fig. 8. TMAE absorption coefficient versus wavelength at various temperatures.

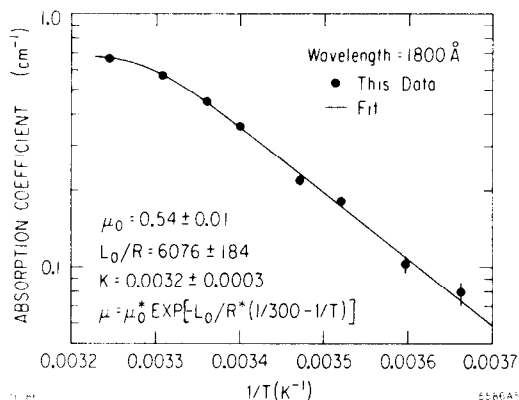


Fig. 9. Clausius-Clapeyron plot of absorption coefficient versus $1/T$ at 1800 Å fitted to Eq. (2).

versus $1/T$. There is obviously some deviation from Eq. (1) at temperatures above 25°C. This is attributed either to the presence of a small amount of stray light within the monochromator or possibly the fluorescence of TMAE within the test cell. We have fitted the data at various wavelengths to the following parameterization which accounts for either of these effects

$$\mu_{obs} = -\frac{1}{D} \ln[(1+k)e^{-\mu D} + k] \quad (2)$$

where D is the length of the transmission cell (8.5 cm) and k represents the fraction of the incident light which is stray (or fluorescence) light. The values of k from the fits are small, typically about 0.003 and constant with wavelength. The values for μ_0 and the slope parameters (L_0/R) are given in Table II. We find the slope parameters to be independent of wavelength, as expected for a pure sample.

The absorption lengths were found to be independent of flow rate through the TMAE bubbler, up to the maximum flow rate examined (42 l/hr).

5. THE BARREL PROTOTYPE

The SLD CRID consists of a barrel and two endcap sections. The barrel's central high voltage plane establishes a drift field of typically 400 V/cm over the full drift box length. Photoelectrons drift towards the detectors at the two ends of the barrel. Each half barrel is divided into 10 azimuthal sectors, each of which contains two drift boxes and their associated liquid radiators and mirrors [Figs. 10(a) and 10(b)]. The drift boxes are 127 cm long and 30 cm wide. Their depth varies from 5.5 cm at the central plane to 9 cm at the detector end.

An engineering prototype is being constructed to investigate various aspects of this design. It will consist of one complete, full-scale 36° sector and a full implementation of the

Table II. Clausius-Clapeyron Parameters from Fit

Wavelength(Å)	μ_0 (cm^{-1})	Slope Parameter (K)
1700	0.56 ±0.01	6214±203
1800	0.54 ±0.01	6077±184
1900	0.64 ±0.01	5995±198
2000	0.478±0.008	6023±176
2100	0.498±0.009	6011±177
2200	0.52 ±0.01	5978±182
2300	0.48 ±0.009	6155±185

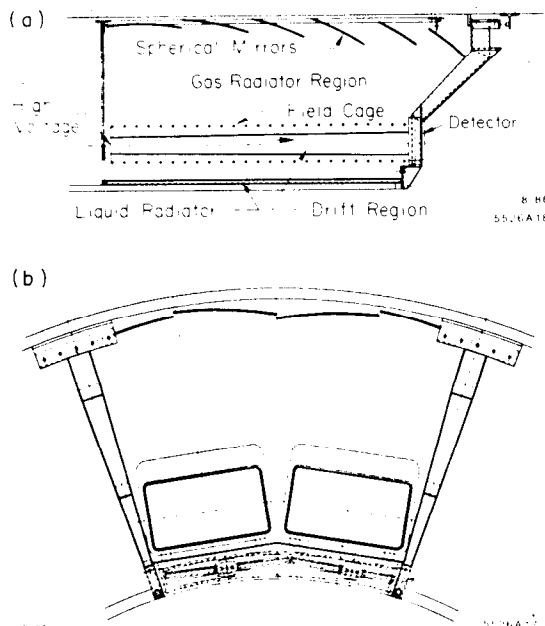


Fig. 10. The Barrel Prototype: (a) one half barrel and (b) one sector.

necessary fluid systems. Various systematic studies connected with this prototype system are now described.

5.1 Gas Radiator Considerations

The chosen gaseous radiator is perfluoro-n-pentane¹³ (C_5F_{12}) at atmospheric pressure. It has a higher refractive index ($n = 1.0017$ at $\approx 2000\text{\AA}$) and better UV transmission than isobutane. It also has the additional advantages of high dielectric rigidity and non-flammability. Unfortunately C_5F_{12} is very electro-negative, which requires the drift boxes, which are surrounded by C_5F_{12} , to be very leak tight. The C_5F_{12} boiling point of 29°C at atmospheric pressure also requires operating the CRID at $\approx 40^\circ\text{C}$.

In order to keep the concentration of C_5F_{12} within the drift boxes below the required 10^{-7} , we have adopted the double-wall drift box construction shown in Fig. 11. In this design, the volume between the inner and outer walls is purged at high flowrate. We estimate that the combination of the double walls and the purge action will reduce the C_5F_{12} leaks into the drift boxes to acceptable levels.

A parallel issue affected by the choice of C_5F_{12} as the radiator gas is the high voltage stability against breakdown. For a nominal drift field of 400 V/cm the maximum potential will be about 55 kV . The concept of our high voltage design is

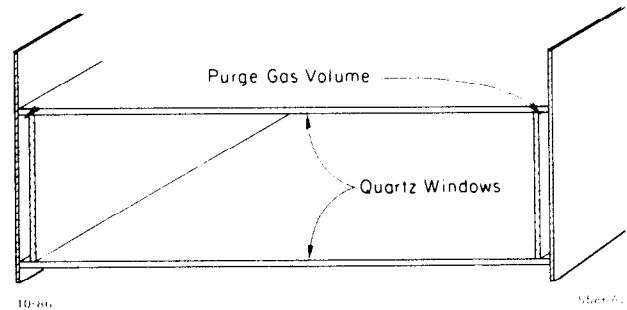


Fig. 11. Double wall drift box.

shown in Figs. 10(a) and 10(b). It does not assume a volume degrader, but instead relies on the large breakdown potential of C_5F_{12} compared to air or hydrocarbons. We have performed tests which indicate that a $4\ \mu\text{A}$ corona in air is reduced by 6 orders of magnitude in a C_5F_{12} atmosphere. A prototype high voltage system has operated continuously without breakdown in air at 80 kV for a period of three months. Our latest tests in a C_5F_{12} atmosphere at 100 kV , almost twice the design value, are similarly encouraging.

5.2 Carbon Fiber Studies

Carbon fibers are a relatively new material for use as anode wires. We have therefore made a number of measurements to determine their mechanical and electrical properties.

The manufacturers¹⁴ quote the following parameters for these fibers: diameter = $7\ \mu\text{m}$, tensile strength = 550 kgf/mm^2 , tensile modulus = $24 \times 10^3\text{ kgf/mm}^2$, density = 1.77 g/cm^3 , thermal expansion coefficient = $-0.1 \times 10^{-6}/^\circ\text{C}$, and electrical resistivity = $1.5 \times 10^{-3}\ \Omega\text{cm}$.¹⁴

We have measured the resistance over a length of 12 cm to be $48.9\text{ k}\Omega$ (average) with an rms of $5.6\text{ k}\Omega$ for a sample of 100 fibers. However, for each individual fiber, the resistivity is very uniform (within 3%) over a length of 25 cm . The fiber breaking tension was measured to be 12.3 g (average) with rms 2.1 g . We have found an anti-correlation between the fiber breaking tension and the electrical resistance. This is consistent with the fluctuations in the breaking tension and resistance being due to variations in the diameters (approximately 5%).

The elongation of fibers has been measured to be 1 mm over a length of 10 cm , when a tension of 10 g was applied. We have found the "elastic curve" very linear and reproducible over many cycles, for a tension below 10 g . Our electrostatic calculations show that a very small tension ($< 2\text{ g}$) is needed to maintain the stability of anode wires in the CRID geometry. Hence, stretching the fibers at a tension of $5\text{--}7\text{ g}$ seems safe, both in terms of the mechanical strength and electrical stability.

Methods of establishing electrical contact between the fiber anodes and the chamber readout are under study. In our physics prototype we soldered nickel-coated fibers onto a PC board frame and then removed the nickel coating with nitric acid. While this method allows a stable electric contact, it is not suitable for mass production; also replacement of wires in an operational detector would be awkward. A more practical method is to use conductive silver epoxy on uncoated carbon fibers. Various brands of conductive epoxies are under study. The H20E epoxy¹⁵ is a promising candidate. When the contact joint is covered with ordinary insulating epoxy, the contact resistivity of the fiber remains stable for a least one month. Longer term stability tests are under way.

We have also investigated the aging properties of these fibers in TMAE saturated gases; these results are reported in another paper at this conference.¹⁶

5.3 Monitoring of the Fluid System

We have developed¹⁷ a simple and inexpensive sonar based instrument which allows us to measure the concentration of

individual gases in gas mixtures. We will use it to continuously check the methane/ethane drift box gas mixture and to monitor the gas mixture within the gaseous radiator enclosure when the nitrogen purge gas is being replaced with C_5F_{12} , or vice versa.

Figure 12 is a general view of the prototype sonar gas analyser. The main component is an 8 cm diameter, 90 cm long cylinder (maintained at a known fixed temperature) containing two ultrasonic transducers.¹⁸ At approximately one second intervals pulses of 45 kHz sound are transmitted through the gas mixture to be detected at the receiving transducer. The speed of sound is obtained from the time delay between the transmitted and received pulses. For these measurements the relative concentrations of the two components were determined by mass flow controllers and independently checked by GC analysis.

Figures 13(a) and 13(b) show the variation in the measured sound velocity as a function of the relative concentrations of

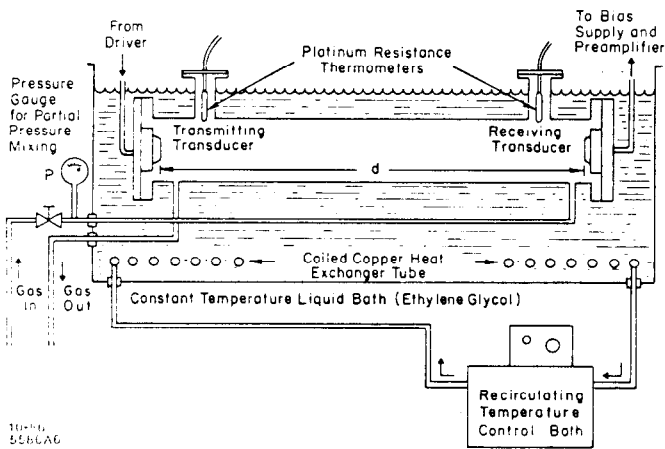


Fig. 12. Prototype sonar gas analyser.

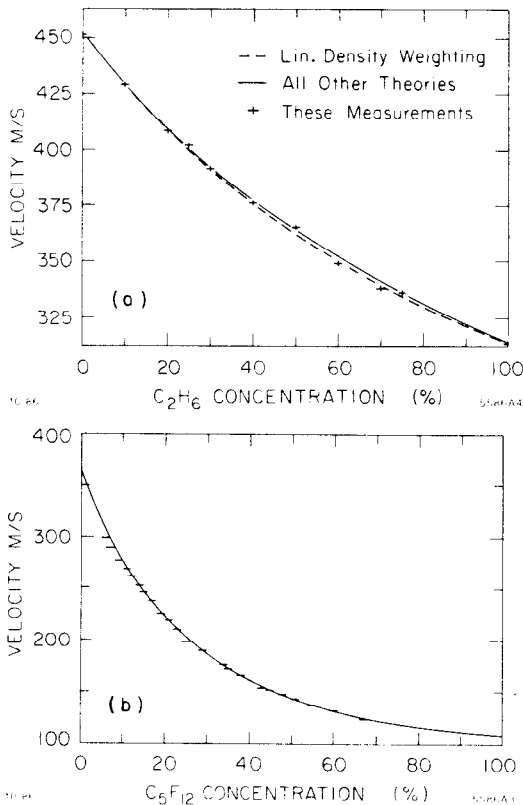


Fig. 13. Variation of sound velocity with gas mixture ratio for (a) methane/ethane at 30°C and (b) nitrogen/ C_5F_{12} at 41°C.

the two components in methane/ethane and nitrogen/ C_5F_{12} mixtures. Our measurements are found to be in good agreement with several empirical and theoretical velocity predictions. With this device, variations in gas composition of the order of 1% are detectable.

6. CONCLUSIONS

We have successfully operated a physics prototype, incorporating the essential features of the SLD CRID design. The measured detector efficiency, the measured resolution using the charge division readout and the measured particle identification capabilities all satisfy the requirements of the SLD CRID. The development of techniques for purifying TMAE and reducing UV absorbing and electronegative contaminants to an acceptable level were crucial to achieving these results.

Our current R&D is directed to the construction of an SLD CRID Barrel Prototype. Some aspects of its design were discussed together with the R&D work involved. Successful testing of the barrel prototype will allow us to begin the SLD CRID construction.

REFERENCES

1. M. Breidenbach, *et al.*, IEEE Trans. Nucl. Sci. NS33, 46 (1986).
2. S. Williams, SLAC-PUB-3360 (1984).
3. S. Williams *et al.*, IEEE Trans. Nucl. Sci. NS32, 681 (1985).
4. V. Ashford *et al.*, IEEE Trans. Nucl. Sci. NS33, 113 (1986).
5. V. Ashford *et al.*, SLAC-PUB-4064 (1986).
6. R. Arnold, *et al.*, Invited talk at Vienna Wire Conf. (1986) LPC/86-09.
7. F. Bird *et al.*, IEEE Trans. Nucl. Sci. NS-33, 261 (1986).
8. N_0 is an efficiency factor which relates the observed number photoelectrons N_{pe} to the radiator thickness (L) and Čerenkov angle (θ_c) by: $N_{pe} = N_0 L \sin^2 \theta_c$.
9. RSA Corp., 690 Saw Mill River Parkway, Ardsley NY 10502.
10. R. A. Holroyd, S. Ehrenson and J. M. Preses, Jour. Phys. Chem. 89, 424 (1985).
11. R. T. Rewick, *et al.* SLAC-PUB-4115 (1986).
12. R. J. Apsimon *et al.*, Nucl. Instr. Meth. A241 339 (1985).
13. C_5F_{12} (PP-50), C_6F_{14} (PP-1) ISC Chemicals, Great Britain.
14. Toho Rayon Co., Tokyo, Japan, BESFIGHT data sheet.
15. Epoxy Technology Inc., 14 Fortune Drive, Billerica MA 01433.
16. J. Va'Vra, these proceedings.
17. G. Hallewell *et al.*, SLAC-PUB-4122 (1986)
18. Polaroid Corp., Instrument Grade Transducers, Part No. 604142.